文章编号：1001-9014(XXXX)XX-0001-06

DOI:10.11972/j.issn.1001-9014.XXXX.XX.001

A Novel W-band Substrate Integrated Microstrip to Ultra-thin Cavity Filter Transition

Cao Yi, Tang Xiaohong, Liu Yong, Cai Zongqi

(1. Yi. Cao, Xiaohong. Tang, Yong. Liu are with the School of Electronic Science and Engineering, University of Electronic Science and Technology of China, Chengdu 611731, China(e-mail: 1921130290@qq.com;
2. xhtang@uestc.edu.cn;
3. liuyong2323@163.com). Zongqi. Cai is with National Key Laboratory of Science and Technology on Reliability Physics and Application of Electronic Component, The Fifth Electronics Research Institute of the Ministry of Industry and Information Technology, Guangzhou, 511370, Guangdong, China(zqcai.uestc@hotmail.com).)

Abstract: A novel substrate integrated microstrip to ultra-thin cavity filter transition operating in the W-band is proposed in this letter. The structure is a new method of connecting microstrip circuits and waveguide filters, and this new structure enables a planar integrated transition from microstrip lines to ultra-thin cavity filters, thereby reducing the size of the transition structure and achieving miniaturization. The structure includes a conventional tapered microstrip transition structure, which guides the electromagnetic field from the microstrip line to the reduced-height dielectric-filled waveguide, and an air-filled matching cavity which is placed between the dielectric-filled waveguide and the ultra-thin cavity filter. The height of the microstrip line, dielectric-filled waveguide and the ultra-thin cavity filter are the same, enabling seamless integration within a planar radio-frequency (RF) circuit. To facilitate testing, mature finline transition structures are integrated at both ends of the microstrip line during fabrication. The simulation results of the fabricated microstrip to ultra-thin cavity filter transition with the finline transition structure, with a passband of 91.5-96.5 GHz, has an insertion loss of less than 1.9 dB and a return loss lower than -20 dB. And the whole structure has also been measured which achieves an insertion loss less than 2.6 dB and a return loss lower than -15dB within the filter´s passband, including the additional insertion loss introduced by the finline transitions. Finally, a W-band compact up-conversion module is designed, and the test results show that after using the proposed structure, the module achieves 95 dBc suppression of the 84 GHz local oscillator. It is also demonstrated that the structure proposed in this letter achieves miniaturization of the system integration without compromising the filter performance.

Key words: **Transition**, **Ultra-thin Cavity filter**, **Planar**, **W-band**, **Miniaturization.**
PACS:

摘要:本文设计了一种W波段基片集成的微带到超薄腔体滤波器的过渡结构。该结构是一种连接微带电路和波导滤波器的新方法,这种新结构实现了从微带线到超薄腔体滤波器的平面集成化过渡,从而减小过渡结构的尺寸,实现小型化。该结构包含一个可以将微带线中的电磁场引入减高介质填充波导的锥形微带过渡结构;一个用于连接减高介质填充波导和超薄腔体滤波器的空气匹配腔。其中,微带线、减高介质填充波导以及超薄腔体滤波器的高度一致,这就使得整个结构可以和射频电路处在同一个平面,从而实现平面集成化。同时,该结构的输入输出端都是微带线,为了便于测试,加工时在该结构两端增加鳍线过渡结构。仿真结果显示,在微带到超薄腔体滤波器过渡结构的两端增加鳍线后,其通带为91.5GHz到96.5GHz,带内插损小于1.9dB,带内回波损耗大于20dB。随后对该结构进行了加工,实测结果显示,其通带为91.5GHz到96.5GHz,带内插损小于2.6dB,带内回波损耗大于15dB。值得注意的是,该测试结果依旧包含了两侧的鳍线所带来的影响。最后,为了验证该结构的可行性,设计了一个紧凑型的W波段集成上变频模块,并用本文设计的结构代替传统的鳍线过渡加波导滤波器结构。经过测试,该W波段集成上变频模块对84GHz的本振抑制达到95dBc,同时证明了本文推荐的结构可以在不影响滤波器性能的前提下实现系统集成的小型化。

Foundation items:Supported by the Fundamental Research Funds for the Central Universities (ZYGX2021J008).

Biography: Yi Cao (2000-), male, Chengdu, master degree candidate. Research area involves microwave and millimetre wave circuits. Email: 1921130290@qq.com.

* **Corresponding author**:Email: liuyong2323@163.com.

关 键 词:过渡结构;超薄腔体滤波器;平面集成化;W波段;小型化

1 Introduction

The role of filters as frequency selection devices in microwave communication systems has attracted significant attention in their design and research. Miniaturization of filters can provide a foundation for the integrated development of microwave communication systems. Therefore, planar integration of filters, as an effective approach to miniaturization, has become a research hotspot in this field. However, W-band filters typically consist of high-Q waveguide designs and are often standalone modules, and this standalone module needs to connect the filter to the RF circuitry via a microstrip-waveguide transition structure.

Various methods and structures for connecting cavity filters to RF circuits have been proposed in recent years, including finline [1], microstrip probes [2], or other specially-shaped transition structures [3-4]. Waveguide-finline-microstrip transition structures utilize fin-shaped metal on both sides of the dielectric substrate to rotate the electric field transmitted in the waveguide by 90 degrees [1, 5-6]. This rotation creates a field discontinuity that will affect circuit matching. Microstrip probe transition structures often have a rectangular waveguide and microstrip line that are perpendicular to each other, which can complicate circuit integration. Specially-shaped structures can enable a straight transition from a microstrip line to a rectangular waveguide, but the bulky structure cannot be used in compact designs. they are bulky and not conducive to circuit miniaturization. These approaches exhibit good performances, but they may not be optimal for compact or planner circuit designs.

To overcome these limitations, substrate-integrated waveguide (SIW) has been employed in filter design, along with transitions from microstrip lines to SIW [7-9], to achieve planar integration of filters with RF circuits. Although SIW-based filters reduce the height and enable planar integration, they occupy a larger area on the plane compared to traditional cavity filters and generate a larger insertion loss.

The aim of this letter is to enable seamless integration within a planar RF circuit while cavity filters are employed. In this letter, a novel substrate integrated microstrip to ultra-thin cavity filter transition with a passband between 91.5-96.5 GHz has been proposed to address the challenges of achieving integrated planar circuit systems. This structure allows for the completion of the entire W-band circuit, including signal input, signal conditioning (including frequency conversion, filtering, and amplification), and signal output, on the same plane.

2 Design Of the Transition and the Filter

Fig. 1 illustrates some details of the geometry of the proposed structure. As shown in Fig. 1, the structure consists of a microstrip line on the left, followed by a traditional tapered microstrip transition, a dielectric-filled waveguide, an air-filled matching cavity, an ultra-thin cavity filter. The structure is symmetrical around the center of the ultra-thin cavity filter.

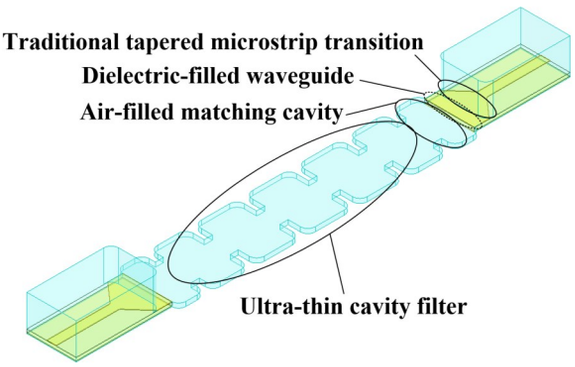

Fig. 1 Structure of substrate integrated microstrip to ultra-thin cavity filter transition.
图1 基片集成的微带到超薄腔体滤波器的过渡结构

Fig. 2 displays the design parameters of the structure from both a top and side view. As shown in Fig. 2, all parts of the proposed circuit are in the same plane except for the air cavity above the microstrip line. The microstrip lines are printed on the Rogers RT/Duroid 5880 with a dielectric constant of 2.2 and a loss tangent of 0.0009. The substrate has a thickness of 0.127mm, while the upper layer metal copper has a thickness of 0.018mm. And the substrate of the dielectric-filled waveguide is also the Rogers RT/Duroid 5880. To simulate the thickness of the silver paste used to adhere the substrate to the cavity during physical assembly, the lower layer metal thickness is set to 0.035mm. The dimensions of the structure are listed in Table 1.

The microstrip line operates in a quasi-TEM mode, as shown in Fig. 3(a), while the dominant mode of transmission in the dielectric-filled waveguide is TE_{10}, depicted in Fig. 3(b). Fig. 3 shows that the electromagnetic field transmitted by the microstrip line is suitable for exciting the electromagnetic field of the rectangular waveguide in its dominant mode. To prevent discontinuities in the electromagnetic field, a tapered microstrip line structure is used to connect the 50-Ohm microstrip line to the dielectric-filled waveguide. This structure has been established through theoretical analysis [10-12].

For a rectangular waveguide operating in the dominant TE10 mode, its transmission characteristics depend solely on its width and are independent of its height. To integrate the dielectric-filled waveguide into the substrate, the height of the waveguide can be made identical to the thickness of the microstrip line. Fig. 4 shows the simulation results for the electric field intensity of the microstrip line, dielectric-filled waveguide and air-filled matching cavity at 94 GHz, which is simulated by using Ansys HFSS.

Fig. 4 demonstrates that the quasi-TEM mode in the microstrip line excites the TE_{10} mode in the dielectric-filled waveguide through the tapered microstrip line, and

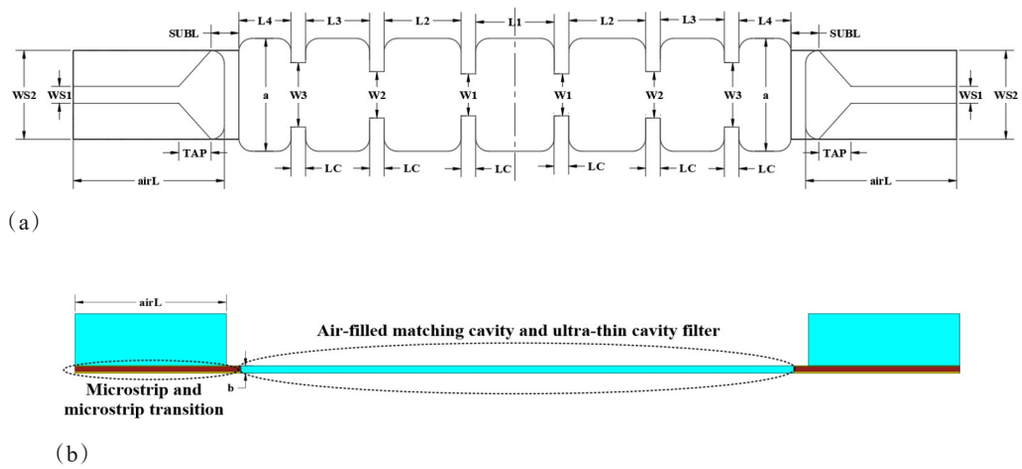

Fig. 2 Design parameters for the proposed transition: (a) top view and (b) side view.
图2 本结构的参数说明:(a)俯视图(b)侧视图

Table 1 Dimensions of the proposed structure (dimensions in mm).
表1 各部分参数

WS1	WS2	W1	W2	W3
0.38	2	0.945	1.045	1.45
L1	**L2**	**L3**	**L4**	**LC**
1.78	1.74	1.45	1.05	0.33
TAP	**SUBL**	**a**	**b**	**airL**
0.72	0.6	2.54	0.18	3.42

Fig. 3 Dominant modal electric field profiles :(a) in microstrip line and (b) in rectangular waveguide.
图3 主要电场分布:(a)微带线电场分布(b)矩形波导电场分布

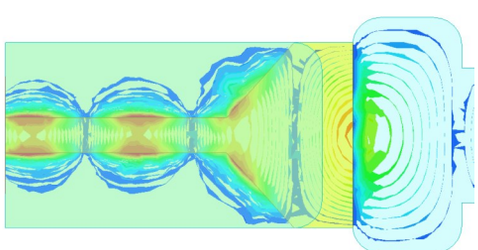

Fig. 4 Simulation results of electric field strength.
图4 电场强度仿真

the TE_{10} mode in the dielectric-filled waveguide excites the TE_{101} mode, the primary resonant mode of the air-filled matching cavity. Through the employment of the dielectric-filled waveguide and the air-filled matching cavity, the transmission of electromagnetic waves from the microstrip line to the ultra-thin waveguide filter is facilitated. Additionally, impedance matching between the microstrip line and the ultra-thin waveguide filter is accomplished by adjusting the dimensional parameters of both the dielectric-filled waveguide and the air-filled matching cavity.

The design of an ultra-thin cavity filter starts with creating a standard-sized filter centered at 94 GHz with a 5 GHz bandwidth. The filter uses an H-plane magnetic coupling approach, and it is constructed by cascading inductive irises with resonant cavities. The iris discontinuity generates higher modes of the electromagnetic field nearby, which cannot propagate in the waveguide. As a result, the magnetic energy near the iris is greater than the electric energy, allowing the iris to function as an inductive structure. Consequently, the inductive iris and its adjacent resonant cavity are treated as an impedance inverter, while the resonant cavity can be modeled as a series resonant circuit. Together, they form the bandpass filter structure of the impedance inverter. Reference [13] shows the design theory for the corresponding coupling matrix, which enables the creation of a filter with standard dimensions.

Conventionally, the three sides of a rectangular resonant cavity are denoted as a, b, and l, with $l>b>a$. The classic electromagnetic field and resonant wavelength equations of the resonant cavity are given in formulas (1), indicating that the resonant characteristics of the cavity are independent of its height, b. In waveguide cavity filters, the resonant mode within the cavity is TE_{101}, which can be easily excited by TE_{10} mode. Therefore, the height of the filter can be reduced to match the height of the dielectric-filled waveguide, enabling connection to the waveguide through an air-filled matching cavity.

$$\begin{cases} E_y = -\dfrac{2\omega\mu_0 a}{\pi} H_0 \sin\left(\dfrac{\pi}{a}x\right)\sin\left(\dfrac{\pi}{l}z\right) \\ H_x = \mathrm{j}2\dfrac{a}{l} H_0 \sin\left(\dfrac{\pi}{a}x\right)\cos\left(\dfrac{\pi}{l}z\right) \\ H_z = -\mathrm{j}2H_0 \cos\left(\dfrac{\pi}{a}x\right)\sin\left(\dfrac{\pi}{l}z\right) \\ E_x = E_z = H_y = 0 \\ \lambda = \dfrac{2}{\sqrt{(1/a)^2 + (1/l)^2}} \end{cases} . \quad (1)$$

Fig. 5 shows the simulation results of the same cavity filters with and without the proposed microstrip to ultra-thin cavity filter transition structure. The 5th order cavity filter without transition structure has an insertion loss (IL) of less than 0.5 dB and a return loss (RL) lower than -26 dB in the 91.5-96.5 GHz passband. However, the ultra-thin cavity filter with the proposed transition structure has an insertion loss of less than 1.5 dB and a return loss lower than -20 dB. Therefore, only 1 dB deterioration because of the added transition structure.

Fig. 6 illustrates the impact of varying the length of the air-filled matching cavity (*L4*) on the structure. It can be observed that the air-filled matching cavity plays important roles in the whole structure. The reason is that the air-filled matching cavity is located between the dielectric-filled waveguide and the first inductive irises of the ultra-thin waveguide filter, and is an important structure for achieving impedance matching of the overall structure. When the variations of *L4* are within ±0.05 mm during simulation, the return loss of the structure changes substantially.

Based on measurement, the traditional finline transition structure is added at the input and output ends of the ultra-thin cavity filter with the proposed transition structure, as shown in Fig. 7. The microstrip structure on the substrate is adhered using silver paste onto the metallized structure. The S-parameters are measured with a Keysight N5224B Vector Network Analyzer, equipped with an external frequency extension module, model N5293AX01.

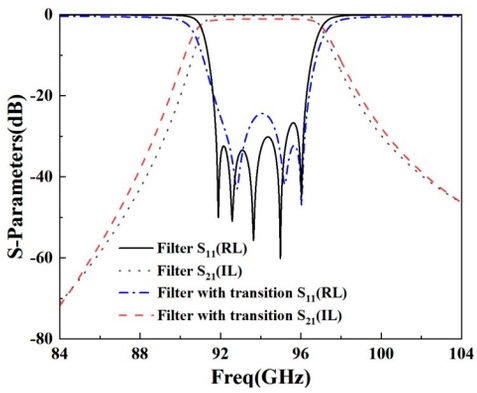

Fig. 5 The simulation results of the same cavity filters with and without the proposed transition structure.
图5 滤波器仿真结果以及增加了过渡结构的滤波器仿真结果

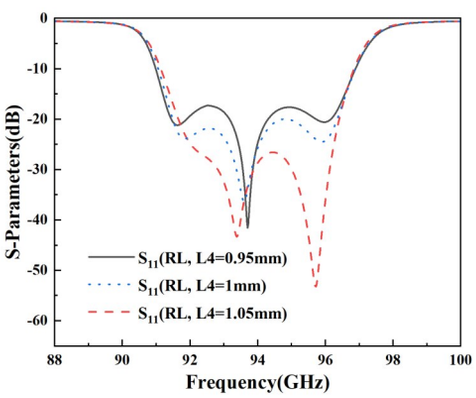

Fig. 6 Impact of varying the length of the *L4*.
图6 L4的长度对整体性能的影响

3 Fabrication and Measurement

Fig. 8 presents the comparison between simulation and test results of the ultra-thin cavity filter with the proposed transition structure and added finline structure. The simulation result shows an insertion loss of less than 1.9 dB and a return loss lower than -20 dB. And the test results indicate an insertion loss of less than 2.6 dB and a return loss lower than -15 dB in the passband of 91.5 to 96.5 GHz. Therefore, the test results are highly consistent with the simulation results. In addition, the inser-

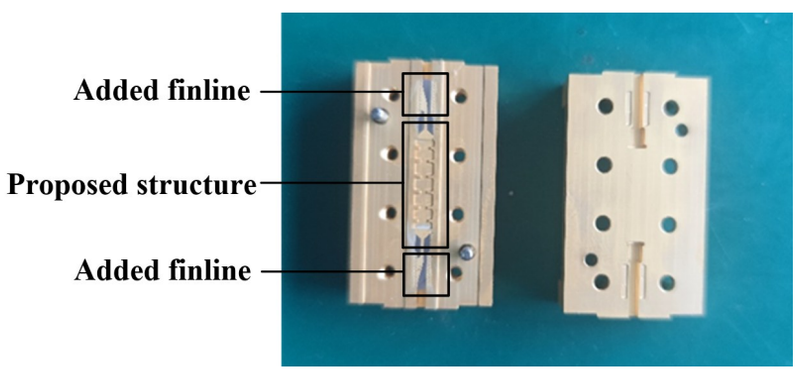

Fig. 7 Photograph of the manufactured structure.
图7 实物加工图

tion loss of the proposed ultra-thin cavity filter needs to subtract the loss introduced by the added finline structure.

Notably, the proposed transition section from the 50 ohms microstrip to the cavity filter, measured 1.36 mm in length, is only about 42% of the length of the centre frequency wavelength, and the height of the ultra-thin cavity filter is only 0.18 mm. Consequently, the structure designed in this letter is highly conducive to the planar integration of RF circuits and cavity filters, which significantly reduces the volume of passive filters in RF circuits and facilitates the miniaturization of RF circuits. Table 2 shows the comparison of the transition part of this work and others.

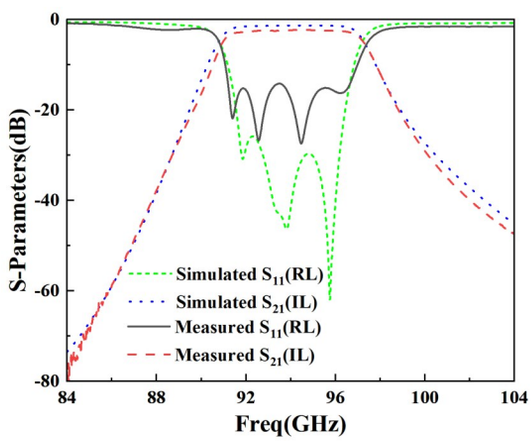

Fig. 8 Measured and simulated result of the structure with the finline structure.
图8 两端增加鳍线过渡的仿真和测试结果

As shown in Table 2, compared with the structures proposed in other references, the proposed structure exhibits a high degree of compactness in terms of its electrical dimensions, particularly in its height, which measures only 0.056λ. Furthermore, it shows an insertion loss of less than 1 dB and a return loss of below -15 dB, outperforming other W-band transition structures in these aspects. This structure is particularly well-suited for the integrated and compact design of W-band circuit structure.

To validate the practicality of the structure designed in this letter, a W-band compact up-conversion module has been fabricated. In the module, a 7th order ultra-thin cavity filter is used instead of the 5th order ultra-thin cavity filter in order to improving local oscillator (LO) suppression. This module inputs a LO signal ranging from 13.75 GHz to 14.25 GHz, which is then frequency-multiplied by multiplier and fed into a mixer as LO. Additionally, an intermediate frequency (IF) signal between 9.5 GHz and 10.5 GHz is also input into the mixer. The mixer subsequently outputs a radio frequency (RF) signal within the range of 92 GHz to 96 GHz. The RF signal is filtered through the structure designed in this letter and subsequently amplified by a low-noise amplifier (LNA) before being output.

After testing, the module's ability to suppress LO at 84 GHz is greater than 95 dBc, which is consistent with the simulation results of a 7th order filter without transition structure connected. In fact, the filtering performance of the structure depends entirely on the performance of the filter connected to the transition structure. A physical prototype of this module is depicted in Fig. 9.

Based on test result, the structure proposed in this letter in the W-band compact up-conversion module not

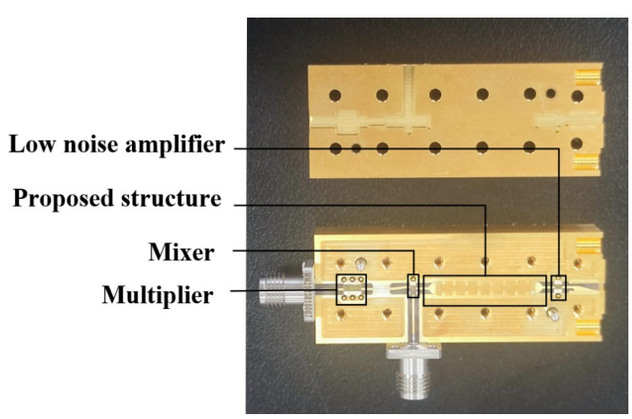

Fig. 9 W-band upconverter module.
图9 W波段上变频模块

Table 2 Comparison of transition of proposed structure and that of other structures.
表2 本结构过渡部分部分与其他结构过渡部分对比

References	[14]	[15]	[16]	This work
Transition type	Microstrip (MS)-Rectangular Waveguide (RWG)	MS-RWG	MS-RWG	MS-Ultra-thin Cavity Filter
Frequency (GHz)	30-40	75-110	27-50	92-96
Length of transition	0.51λ	0.49λ	1.3λ	0.42λ
Height of transition	0.83λ	0.79λ	0.95λ	0.056λ
Insertion loss (dB)	<0.52	<1.29	<3.2	<1
Return loss (dB)	>14.6	>13	>20	>15

only achieves the filtering performance but also achieves miniaturization comparable to traditional finline-to-waveguide filter-to-finline structures. Furthermore, the insertion loss of the entire transition and filtering section is significantly lower than that of traditional ways, demonstrating notable innovation and practicality.

4 Conclusion

This letter presents the design of a novel substrate integrated microstrip to ultra-thin cavity filter transition in the W-band. The structure addresses the challenge of integrating cavity filters into RF circuits in a planar configuration. Importantly, the transition section from the microstrip to the cavity filter is shorter compared to the traditional finline structure, facilitating the miniaturization of RF circuits. Additionally, the structure avoids the need for vertical alignment of the microstrip probes. Therefore, the novelty of this letter lies in the design of a new method of connecting waveguide filters and microstrip circuits, which significantly reduces the insertion loss of the transition structure and facilitates the miniaturization of the transition structure.

References

[1] S. Jing, L. Fa-guo, H. Li-hua, S. Xiao-ying and Z. Yan-qiu, "Waveguide-to-Microstrip Antipodal Finline Transition at W Band," 2013 Third International Conference on Instrumentation, Measurement, Computer, Communication and Control, Shenyang, China, 2013, pp. 510-513.

[2] K. Li, M. Zhao and Y. Fan, "A W band low-loss waveguide-to-microstrip probe transition for millimeter-wave applications, The 2012 International Workshop on Microwave and Millimeter Wave Circuits and System Technology, Chengdu, China, 2012, pp. 1-3.

[3] M. Sarkar and A. Majumder, "A Novel Broadband Microstrip to Waveguide Transition at W band with High Manufacturing Tolerance Suitable for MMIC Packaging," 2018 IEEE MTT-S International Microwave and RF Conference (IMaRC), Kolkata, India, 2018, pp. 1-4.

[4] H. Lee, M. Uhm and I. Yom, "K-band substrate integrated waveguide to rectangular waveguide transition," 2015 Conference on Microwave Techniques (COMITE), Pardubice, Czech Republic, 2015, pp. 1-4.

[5] Xuanxuan Fan, Chao Deng and Rui Zhang, "A new type W-band antipodal-finline transition of waveguide to microstrip based on the HMSIW," 2016 IEEE International Conference on Microwave and Millimeter Wave Technology (ICMMT), Beijing, 2016, pp. 413-415.

[6] R. Bai, Y. -L. Dong and J. Xu, "Broadband Waveguide-to-Microstrip Antipodal Finline Transition without Additional Resonance Preventer," 2007 International Symposium on Microwave, Antenna, Propagation and EMC Technologies for Wireless Communications, Hangzhou, China, 2007, pp. 385-388.

[7] Z. Liu, J. Xu and W. Wang, "Wideband Transition From Microstrip Line-to- Empty Substrate-Integrated Waveguide Without Sharp Dielectric Taper," in IEEE Microwave and Wireless Components Letters, vol. 29, no. 1, pp. 20-22, Jan. 2019.

[8] A. K. Nayak, V. Singh Yadav and A. Patnaik, "Wideband Transition from Tapered Microstrip to Corrugated SIW," 2019 IEEE MTT-S International Microwave and RF Conference (IMARC), Mumbai, India, 2019, pp. 1-4.

[9] Z. Kordiboroujeni and J. Bornemann, "New Wideband Transition From Microstrip Line to Substrate Integrated Waveguide," in IEEE Transactions on Microwave Theory and Techniques, vol. 62, no. 12, pp. 2983-2989, Dec. 2014.

[10] D. Deslandes and K. Wu, "Integrated microstrip and rectangular waveguide in planar form," in IEEE Microwave and Wireless Components Letters, vol. 11, no. 2, pp. 68-70, Feb. 2001.

[11] T. Urakami and Y. Kusama, "A Study on Design of Microstrip Linear Tapered Line Impedance Transformer Using FFT," 2020 IEEE Asia-Pacific Microwave Conference (APMC), Hong Kong, Hong Kong, 2020, pp. 917-919.

[12] M. Kobayashi and N. Sawada, "Analysis and synthesis of tapered microstrip transmission lines," in IEEE Transactions on Microwave Theory and Techniques, vol. 40, no. 8, pp. 1642-1646, Aug. 1992.

[13] R. J. Cameron, C. M. Kudsia, and R. R. Mansour, Microwave Filters for Communication Systems: Fundamentals, Design, Applications. New York: Wiley, 2007.

[14] Z. Dang, Y. Zhang, H. -L. Zhu, B. Yan and R. -M. Xu, "An Isolated Three-Way Power Combiner via Magnetically Coupled Microstrip Ring Probes," in IEEE Transactions on Microwave Theory and Techniques, vol. 72, no. 1, pp. 298-307, Jan. 2024, doi: 10.1109/TMTT.2023.3297409.

[15] B. Zhang, H. Zhu and Y. Zhang, "Wideband In-Line Waveguide-to-Microstrip Transition With Antisymmetric Rectangular Probes," in IEEE Microwave and Wireless Technology Letters, vol. 34, no. 6, pp. 591-594, June 2024, doi: 10.1109/LMWT.2024.3392922.

[16] Cubillos D., Espinoza C., Monasterio D.et al. Design and Optimization of a Broadband Waveguide-to-50 Ω-Microstrip Transition for Q-Band Applications with Low-Loss and Easy Scalability. J Infrared Milli Terahz Waves 44, 693 – 708 (2023). https://doi.org/10.1007/s10762-023-00931-4